J. Phys. Chem. A **2000,** *104,* 5525−5529

Temperature Dependence of Rate Coefficients of Reactions of NO_2 with CH_3S and C_2H_5S

Po-Fu Chang, Tsai T. Wang, and Niann S. Wang*

Department of Applied Chemistry, National Chiao Tung University, 1001, Ta Hsueh Road,
Hsinchu, Taiwan 30010

Yu-Lian Hwang and Yuan-Pern Lee

Department of Chemistry, National Tsing Hua University, 101, Sec. 2, Kuang Fu Road,
Hsinchu, Taiwan 30013

Received: January 24, 2000; In Final Form: April 5, 2000

Rate coefficients of reactions (1) $CH_3S + NO_2$ and (2) $C_2H_5S + NO_2$ were determined using laser photolysis and laser-induced fluorescence. CH_3S and C_2H_5S radicals were generated on photolysis of CH_3SSCH_3 and $C_2H_5SSC_2H_5$, respectively, with a KrF excimer laser at 248 nm. Their concentrations were monitored via fluorescence excited by emission from a dye laser at 371.4 nm (for CH_3S) or 410.3 nm (for C_2H_5S) pumped with a pulsed XeCl excimer laser at 308 nm. Our measurements show that k_1 (297 K) $= (1.01 \pm 0.15) \times 10^{-10}$ cm^3 molecule^{-1} s^{-1} is similar to a value reported by Balla et al. and approximately 50% greater than other previously reported values; listed errors represent 95% confidence limits. Reaction 1 has a negative activation energy: $k_1 = (4.3 \pm 1.3) \times 10^{-11} \exp[(240 \pm 100)/T]$ cm^3 molecule^{-1} s^{-1} for $T = 222-420$ K. Reaction 2 has a rate coefficient similar to reaction 1 at room temperature: k_2 (296 K) $= (1.05 \pm 0.16) \times 10^{-10}$ cm^3 molecule^{-1} s^{-1} but has a small positive activation energy with $k_2 = (2.4 \pm 0.7) \times 10^{-10} \exp[-(210 \pm 80)/T]$ cm^3 molecule^{-1} s^{-1} for $T = 223-402$ K. The temperature dependence of k_2 is determined for the first time. Reactions of NO_2 with HS, CH_3S, and C_2H_5S are compared.

I. Introduction

Reduced sulfur compounds such as CH_3SCH_3, CH_3SH, and CH_3SSCH_3 play an important role in atmospheric chemistry. These compounds are produced biogenically and released into the atmosphere at a rate comparable with emission of SO_2 from human activity.[1,2] Oxidation of these reduced sulfur compounds is initiated primarily through reactions with OH, NO_3, or halogen atoms.[3−5] The CH_3S radical is believed to be the key intermediate[3−6] in these oxidative processes in the atmosphere.[5−12] Although there is no report on atmospheric observation of higher sulfides, one expects that C_2H_5S also plays a role in oxidation of biogenic sulfur compounds; their chemistry is hence critical in an assessment of the final oxidation products and their importance.

Among possible atmospheric reactions of CH_3S and C_2H_5S, the title reactions

$$CH_3S + NO_2 \rightarrow \text{products} \qquad (1)$$

$$C_2H_5S + NO_2 \rightarrow \text{products} \qquad (2)$$

and their reaction with O_3

$$CH_3S + O_3 \rightarrow \text{products} \qquad (3)$$

$$C_2H_5S + O_3 \rightarrow \text{products} \qquad (4)$$

are likely the most important. We have investigated all four reactions using laser photolysis (LP)/laser-induced fluorescence (LIF). Here we report kinetic studies of reactions with NO_2, whereas investigations on reactions involving O_3 will be reported separately.

Reaction 1 was studied by three groups. Balla et al.[13,14] determined the rate coefficients of reactions of CH_3S with NO, NO_2, O_3, and several unsaturated hydrocarbons over the temperature range 295−511 K by means of the LP/LIF technique under pseudo-first-order conditions; they reported $k_1 = (1.06 \pm 0.06) \times 10^{-10}$ cm^3 molecule^{-1} s^{-1}. Tyndall and Ravishankara[15] employed a similar method and reported $k_1 = (6.1 \pm 0.9) \times 10^{-11}$ cm^3 molecule^{-1} s^{-1}. Domine et al.[16] investigated reaction 1 in a discharge-flow system and used a photoionization mass spectrometer to detect CH_3S and other species; their value, $k_1 = (5.1 \pm 0.9) \times 10^{-11}$ cm^3 molecule^{-1} s^{-1} at 297 K and 1 Torr is similar to that of Tyndall and Ravishankara. Later, Turnipseed et al.[17] discovered that CH_3S might form a weakly bound adduct with O_2

$$CH_3S + O_2 \overset{M}{\rightleftharpoons} CH_3SOO \qquad (5)$$

such that under atmospheric conditions, especially at low temperatures, as much as 80% of CH_3S would be in the form of CH_3SOO. Rate coefficient k_6 of the reaction of CH_3SOO with NO_2,

$$CH_3SOO + NO_2 \rightarrow \text{products} \qquad (6)$$

was determined to be $(2.2 \pm 0.6) \times 10^{-11}$ cm^3 molecule^{-1} s^{-1} in a range $T = 227-246$ K. They also reinvestigated[18] reaction 1 in the temperature range 242−350 K and obtained $k_1 = (6.28 \pm 0.28) \times 10^{-11}$ cm^3 molecule^{-1} s^{-1} and its temperature

---

* To whom correspondence should be addressed. E-Mail: nswang@cc.nctu.edu.tw. Fax: 886-3-5723764.

10.1021/jp000294a CCC: $19.00

dependence as $k_1 = (2.06 \pm 0.44) \times 10^{-11} \exp[(320 \pm 40)/T]$ cm^3 molecule^{-1} s^{-1}.

According to the only report on the kinetics of reaction 2, Black et al.[19] determined rate coefficients for the reactions of C_2H_5S with NO_2, NO, and O_2 at 296 K by means of the LP/LIF technique and reported $k_2 = (9.2 \pm 0.9) \times 10^{-11}$ cm^3 molecule^{-1} s^{-1}. Information about the temperature dependence of k_2 is lacking.

In view of large variations in reported values of k_1, and the single measurement on k_2, we studied both reactions 1 and 2. We compare rate coefficients of NO_2 with HS, CH_3S, and C_2H_5S with an objective to understand the effect of alkyl groups in reaction kinetics.

II. Experiments

As the experimental setup and the technique are described in detail previously,[20,21] only a summary is given here. The reaction vessel is a jacketed tube of 40 mm diameter with four sidearms (approximately 15 cm in length) and fitted with Brewster windows. The reaction temperature is regulated on circulating suitable fluid from a thermostated bath through the jacket. CH_3S and C_2H_5S radicals were produced by photolysis of DMDS (dimethyl disulfide, CH_3SSCH_3) and DEDS (diethyl disulfide, $C_2H_5SSC_2H_5$), respectively, with a pulsed KrF excimer laser at 248 nm (5−16 mJ cm^{-2}, 10 Hz). Excess He gas was added to the system and conditions were arranged to ensure that the reactant CH_3S and C_2H_5S were thermalized before detection. CH_3S and C_2H_5S were excited with a dye laser (<10 mJ) pumped by a XeCl excimer laser at 308 nm. For CH_3S the excitation wavelength was set at either 371.4 or 377.0 nm, corresponding to excitation from the ground state $X\ ^2E$ to the $A\ ^2A$ ($v_3' = 1$ or 0) state.[22,23] A filter with passband 450 ± 12 nm or a cutoff filter that passes emission with $\lambda > 450$ nm served to select the wavelength region to be monitored. C_2H_5S was excited from its ground state $^2A'$ to the $B\ ^2A'$ ($v_3' = 2$) state at 410.3 nm.[24,25] Filtered fluorescence in the spectral region 470 ± 5 nm was used to probe its concentration.

The fluorescence was collected perpendicular to both photolysis and probe laser beams with a fused silica lens before detection with a photomultiplier tube (Hamamatsu R955). The signal was integrated over a period 1−2 μs after probe-laser excitation with a gated integrator (Stanford Research Systems, SR245); the scattered light diminished within 1 μs after laser excitation. The background signal, typically ~10% of fluorescence signal, was measured at 75 ms after laser photolysis and subsequently subtracted. The signal was typically averaged over 30−60 laser pulses. The delay between pulses from the photolysis and probe lasers was varied from 10 to 150 μs to construct a temporal profile of CH_3S or C_2H_5S; both lasers were triggered from a pulse/delay generator (Stanford Research Systems, DG535) at a repetition rate of 10 Hz.

He (99.9995%) and O_2 (99.999%) were used without further purification. NO_2, prepared from slow reaction of NO with excess O_2, was stored under O_2 (3 atm) for more than 24 h before use. A mixture (0.98%) of NO_2 in He at a total pressure ~1000 Torr was prepared with standard gas-handling technique. Dimerization of NO_2 (<8%) was taken into account, and the concentration of NO_2 was further calibrated with FTIR spectrometry. DMDS (99%) and DEDS (99%, both from Aldrich) were purified by trap-to-trap distillation and diluted (volumetric ratio 2−4%) in He. Flow rates of carrier gases were measured with mass flow meters (Tylan FM360). Flow rates of DMDS, DEDS, and the NO_2/He mixture were determined on observing the pressure increase in a calibrated volume within a specific period. At low temperature, equilibrium between NO_2 and N_2O_4 was taken into account and the concentration of NO_2 in the reaction vessel was corrected accordingly. At 222 K the correction was ~25% at the highest NO_2 concentration (3.3×10^{14} molecules cm^{-3}, after correction) employed. However, at 234 K the correction decreased to ~8%.

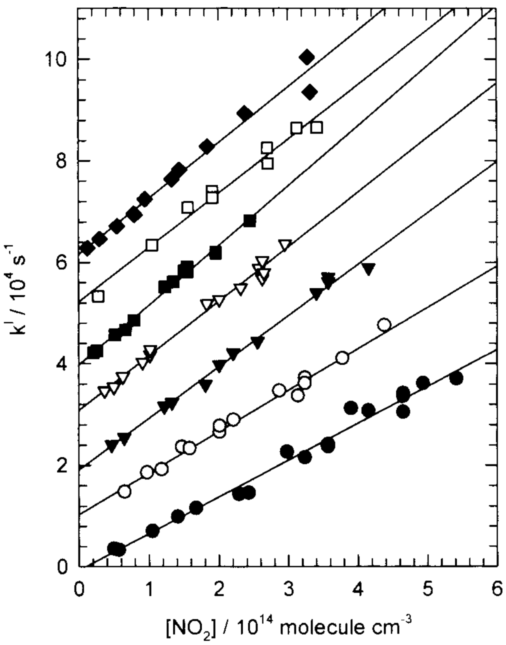

Figure 1. Plots of pseudo-first-order decay rate k^I of CH_3S as a function of [NO_2] at various temperatures: T = 222 K (◆), 234 K (□), 250 K (■), 273 K (▽), 297 K (▼), 346 K (○), and 420 K (●). The ordinates are shifted upward in steps of 10 000 s^{-1} for clarity of depiction.

III. Results and Discussion

The experiments were carried out under pseudo-first-order conditions with [NO_2] ≫ [R] (R = CH_3S and C_2H_5S). Excellent linearity was observed in the semilogarithmic plot of ln [R] vs reaction period. The slope gives the first-order decay rate, k^I, of radicals of interest at a specific [NO_2].

A. Rate Coefficient of the Reaction $CH_3S + NO_2$. Values of k^I for reaction 1 at 297 K are plotted against [NO_2] in Figure 1 (symbol ▼, the ordinate is shifted upward by 20 000 s^{-1} for clarity). The slope yields a bimolecular rate coefficient $k_1 = (1.01 \pm 0.05) \times 10^{-10}$ cm^3 molecule^{-1} s^{-1}; the error represents two standard deviations. The initial concentration of CH_3S, [CH_3S]$_0$, was estimated from the absorption cross section and quantum yield of DMDS (1.24×10^{-18} cm^2 and $\Phi(CH_3S) = 1.80 \pm 0.21$)[26,27] at 248 nm and the fluence of the photolysis laser. In these experiments, [CH_3S]$_0$ = $(0.4-3.3) \times 10^{12}$ molecules cm^{-3}. Variation of [CH_3S]$_0$ (over a factor of 8) or flow velocity (from 4 to 19 cm s^{-1}) or pressure (from 70 to 202 Torr) altered the rate coefficient less than 12%. Systematic error (measurements of flow rates, pressure, and temperature) of our system is estimated to be ~8%[20,21] and error in fitting a slope is ~5%. Hence, we estimate an error approximately 15% for k_1 and recommend a rate coefficient $(1.01 \pm 0.15) \times 10^{-10}$ cm^3 molecule^{-1} s^{-1}.

Rate coefficients k_1 were determined also at 222, 234, 250, 273, 346, and 420 K; these data (k^I vs [NO_2]) are also shown in Figure 1, for which the ordinates are shifted by 60 000, 50 000, 40 000, 30 000, 10 000, and 0 s^{-1}, respectively, for clarity. The experimental conditions and bimolecular rate coefficients k_1 fitted with least squares at various temperatures are listed in Table 1; estimated errors represent two standard

TABLE 1: Experimental Conditions and Bimolecular Rate Coefficients for $CH_3S + NO_2$

T/K	P/Torr	no. expt	$[NO_2]^a/10^{14}$	$k_1{}^b/10^{-11}$
420	70−117	18	0.5−5.5	7.3 ± 0.5^c
346	55−106	14	0.6−4.4	8.2 ± 0.6
297	71−202	12	0.4−4.1	10.1 ± 0.5
273	101	14	0.4−2.9	10.8 ± 0.6
250	101	13	0.2−2.4	11.8 ± 0.6
234	58−106	9	0.3−3.4	12.2 ± 1.0
222	101	12	0.2−3.3	12.0 ± 0.7

[a] In units of molecules cm^{-3}. [b] In units of cm^3 molecule^{-1} s^{-1}. [c] Error limits are 2σ.

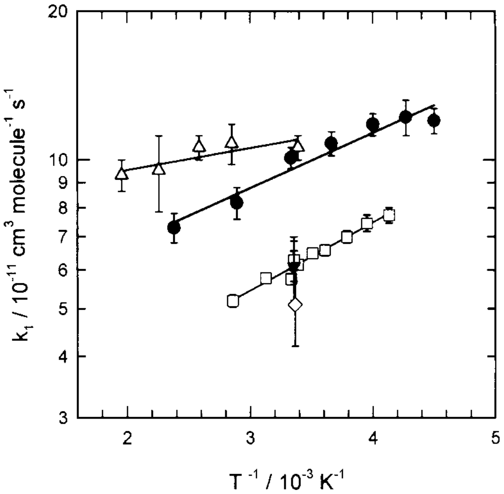

Figure 2. Arrhenius plot of k_1; this work (●); Balla et al.[13] (△); Tyndall and Ravishankara[15] (▼); Domine et al.[16] (◇); Turnipseed et al.[18] (□).

deviations from the fitting. The value of k_1 increases from 7.3 × 10^{-11} to 12.2 × 10^{-11} cm^3 molecule^{-1} s^{-1} as the temperature decreases from 420 to 234 K but remains approximately constant on further decrease to 222 K. Possible condensation of NO_2 on the reactor wall at low temperature might result in a smaller measured value of k_1. However, after careful test of the concentration of NO_2 with FTIR before and after passage through the reaction vessel at low temperature, we found only slight evidence of condensation of NO_2 (<5%). At low temperature, the correction of NO_2 depends significantly on its dimerization equilibrium constant. We employed the recommended value commonly used in stratospheric modeling.[28] When the high-limit of the equilibrium constant was used, the maximum correction increased from 25% to 34% at 222 K; hence k_1 increased from 1.2 to 1.4 × 10^{-10} cm^3 molecule^{-1} s^{-1}.

An Arrhenius plot of k_1 is shown in Figure 2. A fit of these data yields $k_1 = (4.3 \pm 1.0) \times 10^{-11} \exp[(241 \pm 62)/T]$ cm^3 molecule^{-1} s^{-1}; the error limits represent two standard deviations. When the datum at the lowest temperature (222 K) was excluded in the fitting, we obtained $k_1 = (3.8 \pm 0.7) \times 10^{-11} \exp[(278 \pm 48)/T]$ cm^3 molecule^{-1} s^{-1}. Considering possible systematic errors, we report $k_1 = (4.3 \pm 1.3) \times 10^{-11} \exp[(240 \pm 100)/T]$ cm^3 molecule^{-1} s^{-1}.

Rate coefficients k_1 at ambient temperature and their temperature dependence reported previously are compared with our results in Table 2. The value of k_1 at 297 K determined in this work is near that, (1.06 ± 0.06) × 10^{-10} cm^3 molecule^{-1} s^{-1}, reported by Balla et al.[13] Rate coefficients reported by Tyndall and Ravishankara,[15] (6.10 ± 0.90) × 10^{-11} cm^3 molecule^{-1} s^{-1}, and Domine et al.,[16] (5.10 ± 0.90) × 10^{-11} cm^3 molecule^{-1} s^{-1}, are approximately 40−50% smaller. Balla et al.[13] found that the rate coefficient depended on the flow rate in the system, which they interpreted as being due to a heterogeneous reaction between DMDS and NO_2. Tyndall and Ravishankara[15] observed a slight decrease in rate coefficient at large residence periods (~20 s) but only a negligible decrease (<4%) in [DMDS] or production of NO when the reactants were flowed together in the dark. Balla et al. appeared to have used a greater energy (~18 mJ pulse^{-1}) of the photolysis laser. Tyndall and Ravishankara[15] noted that a large concentration of radicals in the work of Balla et al. might account for the difference in k_1. When we employed $[CH_3S]_0$ similar to that in work of Tyndall and Ravishankara, (0.2−1.4) × 10^{12} molecules cm^{-3}, our value of k_1 remained much greater than theirs; the reason for this discrepancy is unclear. The absorption cross section of NO_2 at 248 nm is small; the value $\sigma = 2.75 \times 10^{-20}$ cm^2 molecule^{-1} [27] implies that at most 0.1% of NO_2 is photodissociated. The rate coefficient for the reaction

$$CH_3S + NO \xrightarrow{M} CH_3SNO \qquad (7)$$

is smaller than k_1, with a high-pressure limit $k_\infty = (3.9 \pm 0.6) \times 10^{-11}$ cm^3 molecule^{-1} s^{-1}.[13] For this reason minor photolysis of NO_2 has no effect on measurements of k_1.

The self-reaction of CH_3S,

$$CH_3S + CH_3S \rightarrow \text{other products} \qquad (8)$$

with $k_8 = 4.0 \times 10^{-11}$ cm^3 molecule^{-1} s^{-1} [29] contribute inappreciably to decay of $[CH_3S]$ because $[CH_3S]_0 < 3.3 \times 10^{12}$ molecules cm^{-3}. This is also supported by observation of only a small decay rate (<800 s^{-1}) when no NO_2 was added to the system.

The negative activation energy (E/R = −240 ± 100 K) determined in this work is similar to that (−320 ± 40 K) reported by Turnipseed et al.,[18] with error limits overlapping each other. The value E/R = −81 K reported by Balla et al.[14] is slightly smaller. All three reports indicate a small negative temperature dependence of k_1; the agreement is satisfactory.

According to previous work[15,16] CH_3SO and NO are the primary products of reaction 1

$$CH_3S + NO_2 \rightarrow CH_3SO + NO \qquad (1a)$$

with quantum yields $\Phi(NO) = 0.8 \pm 0.2$ and $\Phi(CH_3SO) = 1.07 \pm 0.15$. No direct evidence for the termolecular combination or for abstraction of H

$$CH_3S + NO_2 \xrightarrow{M} CH_3SNO_2 \qquad (1b)$$

$$CH_3S + NO_2 \rightarrow H_2CS + HONO \qquad (1c)$$

was found in previous kinetic studies. However, experiments in smog chambers indicated production of CH_3SNO_2 as a minor product.[30] Whether CH_3SNO_2 was produced directly from reaction 1b or from other reactions is unclear. That k_1 is independent of both the pressure and nature of carrier gas is consistent with CH_3SO and NO being major products.

The product CH_3SO may react further with NO_2 and produce secondary NO,

$$CH_3SO + NO_2 \rightarrow CH_3SO_2 + NO \qquad (9)$$

Tyndall and Ravishankara[15] observed [NO] to increase with two components with time constants separated by a factor ~10. They also observed fluorescence resulting from a distinct species of which the temporal profile is consistent with that predicted for CH_3SO_2. On modeling observed temporal profiles of NO, they

TABLE 2: Comparison of Rate Coefficients of Reactions of NO_2 with HS, CH_3S, and C_2H_5S

	k at ambient T						
reactant	$k/10^{-11}$	*T*/K	$A/10^{-11}$	(E/R)/K	*T*/K	method[a]	reference
HS	6.7 ± 1.0	295	2.9 ± 0.5	-240 ± 50	221−415	DF-LMR	Wang et al.[30]
	4.8 ± 1.0	298				LP-LPA	Stachnik & Molina[31]
CH_3S	10.1 ± 1.5	297	4.3 ± 1.3	-240 ± 100	222−420	LP-LIF	this work
	6.28 ± 0.28	298	2.06 ± 0.44	-320 ± 40	242−350	LP-LIF	Turnipseed et al.[18]
	10.8 ± 1.0	295	8.3 ± 1.4	-81 ± 50	295−511	LP-LIF	Balla et al.[13]
	5.1 ± 0.9	297				DF−PIMS	Domine et al.[16]
	6.10 ± 0.90	298				LP-LIF	Tyndall & Ravishankara[15]
C_2H_5S	10.5 ± 1.6	296	24 ± 7	210 ± 80	223−402	LP-LIF	this work
	9.2 ± 0.9	296				LP-LIF	Black et al.[19]

[a] DF = discharge-flow; LMR = laser magnetic resonance; LP = laser photolysis; LPA = long-path absorption; LIF = laser-induced fluorescence; PIMS = photoionization mass spectrometry.

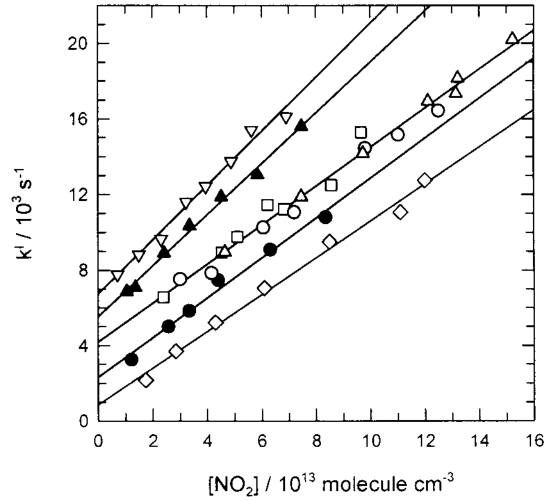

Figure 3. Plots of pseudo-first-order decay rate of C_2H_5S as a function of $[NO_2]$ at $T = 230$ K (◇), 269 K (●), 296 K [(□) 65 Torr; (○) 213 Torr; (△) 484 Torr], 348 K (▲), and 402 K (▽). For clarity the ordinates are shifted uprard in steps of 2000 s^{-1}, respectively.

TABLE 3: Experimental Conditions and Bimolecular Rate Coefficients for $C_2H_5S + NO_2$

T/K	*P*/Torr	no. expt	$[NO_2]^a/10^{13}$	$k_2^{b,c}/10^{-10}$
402	110	8	0.7−6.9	1.45 ± 0.14
372	100−111	9	0.7−6.8	1.39 ± 0.16
348	106	7	1.0−7.5	1.39 ± 0.09
319	67	6	1.2−8.8	1.23 ± 0.16
296	65−484	21	2.2−15.2	1.05 ± 0.06
288	65	8	1.3−9.6	1.09 ± 0.10
269	66	6	1.3−10.0	1.06 ± 0.13
253	65	8	1.8−12.2	1.05 ± 0.13
238	65	8	2.1−11.8	1.01 ± 0.08
230	66	7	1.7−12.0	0.99 ± 0.06
223	66	7	1.9−10.6	0.96 ± 0.04

[a] In units of molecules cm^{-3}. [b] In units of cm^3 $molecule^{-1}$ s^{-1}. [c] Error limits are 2σ.

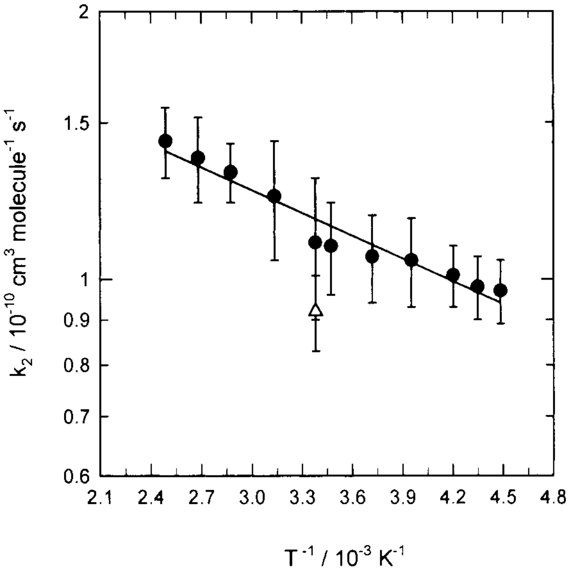

Figure 4. Arrhenius plots of k_2; this work (●); Black et al.[19] (△).

obtained $k_9 = (8 \pm 5) \times 10^{-12}$ cm^3 $molecule^{-1}$ s^{-1}, about one-tenth of k_1. This secondary reaction does not affect k_1 measured on monitoring the decay of $[CH_3S]$ in our work.

B. Rate Coefficient of the Reaction $C_2H_5S + NO_2$. C_2H_5S was produced from photolysis of DEDS at 248 nm. The rate coefficients of reaction 2 were determined at 11 temperatures in a range 223−402 K. Representative plots of k^I vs $[NO_2]$ are shown in Figure 3 for $T = 230$, 253, 296, 348, and 402 K. The data obtained at various pressures are indicated for 296 K. The slope of each line yields k_2 at a particular temperature. Table 3 summarizes experimental conditions and k_2 at various temperatures; the error limits represent 2σ from a fit with least squares. At 296 K, $k_2 = (1.05 \pm 0.06) \times 10^{-10}$ cm^3 $molecule^{-1}$ s^{-1}. Taking into account possible systematic errors, we report $k_2 = (1.05 \pm 0.16) \times 10^{-10}$ cm^3 $molecule^{-1}$ s^{-1} at 296 K. The rate coefficient decreases slightly as temperature decreases from 402 to 223 K. An Arrhenius plot of k_2 is shown in Figure 4. A least-squares fit yields $k_2 = (2.38 \pm 0.31) \times 10^{-10} \exp[-(207 \pm 36)]/T]$ cm^3 $molecule^{-1}$ s^{-1}, in which error limits represent two standard deviations from the fit. Considering possible systematic errors, we report $k_2 = (2.4 \pm 0.7) \times 10^{-10} \exp[-(210 \pm 80)/T]$ cm^3 $molecule^{-1}$ s^{-1}.

For the single reported determination of k_2, Black et al.[19] studied the kinetics of reaction 2 at 296 K with a technique similar to ours. Both C_2H_5SH and DEDS served as precursors of C_2H_5S. They observed slight regeneration of C_2H_5S when C_2H_5SH was used to produce C_2H_5S and $[NO_2]/[C_2H_5SH]$ was small. The reason is that H atoms produced from photolysis of C_2H_5SH react with NO_2 to form OH, which subsequently reacts with C_2H_5SH to regenerate C_2H_5S. When they used DEDS as a precursor or used $[NO_2]/[C_2H_5SH] \approx 133$, such an interference was diminished. They obtained $k_2 = (9.2 \pm 0.9) \times 10^{-11}$ cm^3 $molecule^{-1}$ s^{-1}, which agrees with our value within quoted error limits.

The temperature dependence of k_2 is determined for the first time. It shows a small positive activation energy in contrast with k_1 that has a negative activation energy.

C. Comparison of Reactions of NO_2 with HS, CH_3S, and C_2H_5S. For reactions of NO_2 with HS, CH_3S, and C_2H_5S, rate coefficients at ambient temperature and their temperature dependence are compared in Table 2. Rate coefficients of reactions of CH_3S and C_2H_5S are nearly identical, and slightly greater than that for HS,[28,31,32] but the activation energy varies from $E/R \sim (-240)$ K for HS and CH_3S to ~210 K for C_2H_5S.

Although formation of HSO (or CH_3SO) and NO is identified as the major channel,

$$HS + NO_2 \rightarrow HSO + NO \tag{10a}$$

$$CH_3S + NO_2 \rightarrow CH_3SO + NO \tag{1a}$$

the small negative temperature dependence indicates that the reactions probably proceed through formation of an adduct that decomposes readily. The most likely adducts are HSONO and CH_3SONO. A finite activation energy is expected for formation of HSO (or CH_3SO) + NO from $HSNO_2$ (or CH_3SNO_2). If we assume that HS and CH_3S react via similar paths, a greater preexponential factor (A) is expected for reaction 1a. Our value of $(4.3 \pm 1.3) \times 10^{-11}$ is consistent with such expectation. The value (2.06×10^{-11}) reported by Turnipseed et al.[18] for reaction 1a is smaller than that (2.9×10^{-11}) reported for reaction 10a.

Because no product analysis was performed for reaction 2, we cannot explain definitively why the temperature dependence becomes positive as the reactant varies from CH_3S to C_2H_5S. One possibility is that the H-abstraction channel (reaction 2b) becomes more important in this case,

$$C_2H_5S + NO_2 \rightarrow C_2H_5SO + NO \tag{2a}$$

$$\rightarrow (CH_3)CHS + HONO \tag{2b}$$

so that its positive temperature dependence contributes more to the apparent rate coefficient than in cases of HS and CH_3S. Further experiments are needed to confirm this postulate.

D. Implications for Atmospheric Chemistry. On the basis of present kinetic data, reaction 1 is negligible in the clean marine troposphere because a mixing ratio with NO_2 at 100−300 ppt gives a loss rate of 0.3−0.8 s^{-1} for CH_3S.[3] However, in polluted regions in which NO_x concentrations can reach to the ppb level, reaction 1 becomes as important as reaction 3.[33] The greater value of k_1 determined in this work increases the relative importance of reaction 1 in oxidation of CH_3S in polluted air.

Rate coefficients for reactions of C_2H_5S with NO_2 and O_3,

$$C_2H_5S + NO_2 \rightarrow \text{products} \tag{2}$$

$$C_2H_5S + O_3 \rightarrow \text{products} \tag{4}$$

are $k_2 = (1.05 \pm 0.16) \times 10^{-10}$ and $k_4 = (7.2 \pm 1.0) \times 10^{-12}$ cm^3 $molecule^{-1}$ s^{-1},[34] respectively. The rate of loss of C_2H_5S through reaction with NO_2 is similar to that of CH_3S at room temperature, but it decreases at low temperatures because of its positive temperature dependence. The ratio k_2/k_4 for C_2H_5S is near k_1/k_3 for CH_3S at 297 K, indicating that reaction 2 is unimportant in the clean air, similar to the case of CH_3S.

Acknowledgment. We thank the National Science Council of the Republic of China (grants no. NSC89-2119-M-007-001 and NSC89-2113-M-009-010) for support.

References and Notes

(1) Bates, T. S.; Lamb, B. K.; Guenther, A.; Dignon, J.; Stoiber, R. E. *J. Atmos. Chem.* **1992**, *14*, 315.

(2) Spiro, P. A.; Jacob, D. J.; Logan, J. A. *J. Geophys. Res.* **1992**, *97*, 6023.

(3) Tyndall, G. S.; Ravishankara, A. R. *Int. J. Chem. Kinet.* **1991**, *23*, 483.

(4) (a) Atkinson, R.; Pitts, J. N., Jr.; Aschrnann, S. M. *J. Phys. Chem.* **1984**, *88*, 8, 1584. (b) MacLeod, H.; Aschmann, S. M.; Atkinson, R.; Tuazon, E. C.; Sweetman, J. A.; Winer, A. M.; Pitts, J. N., Jr. *J. Geophys. Res.* **1986**, *91*, 5338.

(5) (a) Yin, F.; Grosjean, D.; Seinfeld, J. H. *J. Atmos. Chem.* **1990**, *11*, 309. (b) Yin, F.; Grosjean, D.; Flagan, R. C.; Seinfeld, J. H. *J. Atmos. Chem.* **1990**, *11*, 365.

(6) Wine, P. H.; Kreutter, N. M.; Gump, C. A.; Ravishankara, A. R. *J. Phys. Chem.* **1981**, *85*, 2660.

(7) Hynes, A. J.; Wine, P. H. *J. Phys. Chem.* **1987**, *91*, 3672.

(8) MacLeod, H.; Jourdain, J. L.; Poulet, G.; LeBras, G. *Atmos. Environ.* **1984**, *18*, 2621.

(9) Niki, H.; Maker, P. D.; Savage, C. M.; Breitenbach, L. P. *Int. J. Chem. Kinet.* **1983**, *15*, 647.

(10) Hatakeyama, S.; Akimoto, H. *J. Phys. Chem.* **1983**, *87*, 2387.

(11) Grosjean, D. *Environ. Sci. Technol.* **1984**, *18*, 460.

(12) Jensen, N. R.; Hjorth, J.; Lohse, C.; Skov, H.; Restelli, G. *J. Atmos. Chem.* **1992**, *14*, 95.

(13) Balla, R. J.; Nelson, H. H.; McDonald, J. R. *Chem. Phys.* **1986**, *109*, 101.

(14) Balla, R. J.; Weiner, B. R.; Nelson, H. H. *J. Am. Chem. Soc.* **1987**, *109*, 4804.

(15) Tyndall, G. S.; Ravishankara, A. R. *J. Phys. Chem.* **1989**, *93*, 2426.

(16) Domine, F.; Murrells, T. P.; Howard, C. J. *J. Phys. Chem.* **1990**, *94*, 5839.

(17) Turnipseed, A. A.; Barone, S. B.; Ravishankara, A. R. *J. Phys. Chem.* **1992**, *96*, 7502.

(18) Turnipseed, A. A.; Barone, S. B.; Ravishankara, A. R. *J. Phys. Chem.* **1993**, *97*, 5926.

(19) Black, G.; Jusinski, L. E.; Patrick, R. *J. Phys. Chem.* **1988**, *92*, 5972.

(20) Diau, E. W.-K.; Tso, T.-L.; Lee, Y.-P. *J. Phys. Chem.* **1990**, *94*, 5261.

(21) You, Y. Y.; Wang, N. S. *J. Chin. Chem. Soc.* **1993**, *40*, 337.

(22) Chiang, S.-Y.; Lee, Y.-P. *J. Chem. Phys.* **1991**, *95*, 66.

(23) Suzuki, M.; Inoue, G.; Akimoto, H. *J. Chem. Phys.* **1984**, *81*, 4505.

(24) Black, G.; Jusinski, J. E. *Chem. Phys. Lett.* **1988**, *136*, 241.

(25) Hung, W.-C.; Shen, M.-y.; Yu, C.-h.; Lee, Y.-P. *J. Chem. Phys.* **1996**, *105*, 5722.

(26) Hearn, C. H.; Turcu, E.; Joens, J. A. *Atmos. Environ.* **1990**, *24A*, 1939.

(27) Schneider, W.; Moortgat, G. K.; Tyndall, G. S.; Burrows, J. P. *J. Photochem. Photobiol.* **1987**, *40*, 195.

(28) DeMore, W. B.; Sander, S. P.; Golden, D. M.; Hampson, R. F.; Kurylo, M. J.; Howard, C. J.; Ravishankara, A. R.; Kolb, C. E.; Molina, M. J. *Chemical Kinetics and Photochemical Data for Use in Stratospheric Modeling*; JPL Publication 97-4; Jet Propulsion Laboratory: Pasadena, CA, 1997.

(29) Anastasi, C.; Broomfield, M.; Nielson, O. J.; Pagsberg, P. *Chem. Phys. Lett.* **1991**, *182*, 643.

(30) Barnes, I.; Bastian, V.; Becker, K. H.; Niki, H. *Chem. Phys. Lett.* **1987**, *140*, 451.

(31) Wang, N. S.; Lovejoy, E. R.; Howard, C. J. *J. Phys. Chem.* **1987**, *91*, 5743.

(32) Stachnik, R. A.; Molina, M. J. *J. Phys. Chem.* **1987**, *91*, 4603.

(33) Mihalopoulos, N.; Nguyen, B. C.; Boissard, C.; Campin, J. M.; Putaud, J. P.; Belviso, S.; Barnes, I.; Becker, K. H. *J. Atmos. Chem.* **1992**, *14*, 459.

(34) Lin, J. T.; Chew, E. P.; Wang, T. T.; Wang, N. S.; Lee, Y. Y.; Chen, I. C.; Lee, Y. P. To be published.